SED-Vol. 14, Wind Energy
ASME 1993

FATIGUE PERFORMANCE OF WIND TURBINE BLADE COMPOSITE MATERIALS

John F. Mandell, Robert M. Reed,
Daniel D. Samborsky, and Qiong (Rena) Pan
Department of Chemical Engineering
Montana State University
Bozeman, Montana

ABSTRACT

The fatigue behavior of generic materials used in wind turbine blades has been explored. Coupon testing was carried out under constant amplitude fatigue loading to beyond 10^7 cycles for most materials. Unidirectional materials preformed close to expectations despite fiber misalignment. Materials with triaxial ($0^0/\pm 45^0$) reinforcement showed greater fatigue sensitivity than expected, but lifetime trends flattened at high cycles. The uniaxial and triaxial materials could be normalized to a single S-N lifetime trend for each case.

Results include the effects of differing matrix materials, manufacturing methods, rein-forcement structure, loading conditions, and specimen edge effects.

INTRODUCTION

The high cycle fatigue resistance of composite materials used in wind turbine rotor blades has been recognized as a major uncertainty in predicting the reliability of wind turbines over their design lifetime [1]. Blades are expected to experience 10^8 to 10^9 significant fatigue cycles over a 20 to 30 year lifetime, well beyond the cycle range where the fatigue behavior of composites has previously been investigated. For the lower cost glass fiber composites used in wind turbine blades, there exists neither an adequate data base at high cycles [1], nor an adequate lifetime prediction methodology proven for composite structures in general [2].

BACKGROUND

The fatigue behavior of composite materials has been the subject of several reviews [1-7], and is distinguished by several important general features [2, 3]:

1. Failure is usually progressive, resulting from the gradual accumulation and interaction of dispersed damage, rather than by the nucleation and growth of a dominant crack.
2. As damage accumulates, the constitutive relations of the material may change significantly.
3. A number of distinct damage modes can be identified, including fiber dominated tension and compression, matrix dominated cracking parallel to the fibers, and interlaminar cracking between plies. Some of these damage modes may produce failure directly, particularly fiber dominated modes, while modes such as matrix cracking may have an indirect effect on failure by causing load transfer onto the fibers.

This work was supported by the U.S. Department of Energy and Sandia National Laboratories under subcontract 40-8875, and the National Renewable Energy Lab under subcontract XF-1-11009-5. Materials were supplied by Phoenix Industries and U.S. Windpower.

4. Under tensile loading, the strains to produce matrix cracking in off-axis plies (with thermoset resin composites) are generally well below those to produce fiber failure. As a consequence, in multidirectional composites, cracking tends to initiate first in domains (plies) where the fibers are at the greatest orientation relative to the maximum tensile stress. Cracking accumulates in these domains (such as 90^0 plies), followed by domains of lesser orientation (such as 45^0 plies). Delamination between piles may also occur at cut edges, ply terminations, or at the intersection of matrix cracks in adjoining plies. Finally, gross failure often occurs by fiber breakage in any domains oriented nearly parallel to the maximum stress (such as 0^0 plies). Under compressive loading the strains to produce matrix cracking in off-axis domains are often comparable to those for fiber dominated failure, so damage development in a matrix dominated mode may also produce gross failure.

5. Large-scale delamination between plies has been a significant failure mode for composite structures, particularly with out-of-plane loads. Classical linear elastic fracture mechanics has proven applicable to delamination problems under different modes of crack extension and for both static and fatigue loading.

6. Theoretical models for damage progression and failure are under development, but no general approach to lifetime prediction for composites is widely accepted. Only delamination failures have a well developed theoretical context in classical fracture mechanics.

7. Few results are available for lifetimes greater than 10^6 cycles for any composite systems. Cumulative damage effects from varying load histories have been studied in only a few cases, and no general theoretical framework (such as linear damage laws) is accepted.

While these features are common to a broad range of fiber and matrix systems with continuous or chopped strand reinforcement, the actual sensitivity to fatigue loads depends strongly on the material system used, particularly the type of fiber and style of reinforcement (parallel aligned layers, woven, chopped, etc.). S-N lifetime data (maximum stress vs. cycles to failure) can follow a variety of trends [8,9]. One trend that is frequently observed takes the form

$$S/S_0 = 1\text{-}b \log N \qquad (1)$$

or

$$S/S_0 = N^{-(1/m)} \qquad (2)$$

where S is the maximum stress, S_0 is the single cycle (static) strength, N is the number of cycles to failure, and m and b are material constants. Eq.(1) yields a linear S-N curve on a plot of S vs. log N while Eq.(2) is linear on a log-log plot. Eq.(2) derives from integration of the Paris fatigue crack growth law

$$da/dN = A\,(K_{max})^m \qquad (3)$$

where a is the crack length, K_{max} is the maximum stress intensity factor (K is more commonly used) and A is a constant; m should be the same as in Eq. 2.

Empirical findings are that S-N data for composites may show a better fit to either Eq.(1) or (2) depending on the material system, and in many cases it is difficult to distinguish which is the more representative form. Com-posites with well aligned fibers either parallel to the (uniaxial) load direction, or at some orientation, tend to follow Eq. (1) closely. Composites with multi-directional reinforcement where the lifetime is clearly dominated by one orientation also follow Eq. (1)[8].

However, more complex cases such as woven fabrics and chopped strand composites tend to have nonlinear S-N curves on a semi-log plot, and the most appropriate curve fit is unclear. Woven fabric reinforcements show an even more nonlinear trend on a semi-log plot, with a steep curve atlow to moderate cycles associated with delamination at the weave cross-over points [5], while the curves tend to flatten at higher cycles; significant high cycle data are not available.

Fatigue crack growth data for thermoset composites and neat resins tend to show very high exponents, m (Eq. 2 & 3), compared with most metals, representing increased fatigue resistance. Values reported for m for both the neat matrix materials and opening-mode delamination are often in the 10-20 range. For Mode II the exponents tend to be in the range of 10-12 [8].

EXPERIMENTAL METHODS

Materials were supplied by U.S. wind industry blade manufacturers, molded as flat sheets using preparation methods representative of blade manufacturing. This involved hand layup using nonwoven (stitched) E-glass fabrics having either unidirectional or triaxial ($0^0/\pm 45^0$) fibers. The triaxial reinforcement contained unidirectional layers stitched together, having differing amounts of 0^0 and $\pm\ 45^0$ material. The directions given refer to the angle of the fibers relative to the direction of the uniaxial stress which is applied to test specimens cut from the sheets, so that the 0^0 indicates that the fibers are approximately parallel-aligned in the direction of the applied stress.

Table 1 gives a description of each material used in this study. The materials were intended to be as represen-tative of wind turbine blades as possible, including typical fiber misalignments. However, to maintain reasonable specimen to specimen consistency, regions of material with greater than 4^0 fiber misalignment were excluded in preparing test specimens.

The materials in Table 1 contain several different reinforcement styles, two generic types of matrix materials (unsaturated polyester and unsaturated vinylester), and differing processing methods from the two manufacturers. Materials F, G, H and J also contain ply terminations to represent regions of blades which taper in thickness, the results of which will be reported elsewhere.

Flat coupons were used throughout the study, following ASTM D 3039-76 as closely as possible. The flat rectangular specimens were cut with a diamond-edged saw from larger sheets supplied by blade manufactures. Tabs for gripping were bonded to the ends with an epoxy adhesive cured at room temperature or 140^0F. (The original material sheets experienced exotherms in excess of 140^0 and some were

post cured at 140^{0}F.) A variety of adhesives and tab materials were investigated. Most of the specimens were prepared with epoxy electrical vector board (Radio Shack Protoboard) which worked well in most cases.

Compression and reversed loading tests used a similar geometry, but with a much shorter gage length than for tension. Particular gage lengths for compression specimens were empirically selected to prevent elastic buckling in the undamaged state. No side constraint was used.

Tests were run on a 50 kip capacity MTS 880 servohydraulic testing machine using hydraulic grips. A constant amplitude, force control, sine waveform loading was used in all cases. The frequency was varied approximately inversely with the maximum stress level to maintain a constant load rate. The frequency at low cycles was a few Hz, varying up to 15 Hz for the highest cycle tests. This frequency range was the fastest possible without overheating the specimens. Fatigue lifetime is generally not found to be sensitive to frequency in the absence of thermal runaway hysteretic heating [8].

Strain measurements at higher cycles were a problem. Bonded strain gages failed, and fatigue extensometers did not always remain well seated. Cyclic stress-strain and modulus data were obtained by interrupting the tests and replacing the extensometer; thus, the cumulative strain, where it was measured, was small. Other test interruptions occurred due to power failures. These were common in very long tests, and the testing equipment did not generally overload the specimens significantly during shut-downs. Peak loads during shut-downs were recorded.

All tests were conducted in ambient laboratory air. These ambient conditions are generally low humidity with temperatures between 65 and 80^{0}F.

Further details of the results of this study can be found in Ref. 9.

RESULTS AND DISCUSSION

Unidirectional Materials

Materials A, B, and L are unidirectional, loaded in the longitudinal (fiber) direction. Materials A and B differ only in matrix material (polyester vs vinylester); L is constructed with slight fiber misalignment between strands and layers, and has a higher fiber content.

Figure 1 gives S-N data for material B. The arrows on the points at 40 x 10^6 cycles indicate"run-out" tests which did not fail. Several aspects of Figure 8 are significant:

1. The data at higher stresses fall below Eq. 1 with a slope, b, of 0.1 (10%/ decade).
2. The power law fit of Eq. 2 is in good agreement with the data for an exponent, m, of 13.5.
3. There is no apparent effect of specimen width for the 1.0 and 2.0-inch-wide specimens tested.
4. The initial strain value shown on the right side of the graph, 0.68%, corresponds to the 20 ksi stress level. The strain increases slightly during the specimen lifetime.

Materials A, B and L are compared in Figure 2, with the maximum stress, S, normalized by the static strength, S_0. Again, Eq.(2) with a power law exponent in the range of m=13.5 fits the data well. Little difference in the normalized S-N curve for unidirectional Materials A, B, and L is noted, despite the differences in matrix material and manufacturing processes. The vinylester matrix typically yields a slightly higher static strength [9] , but little difference in fatigue, particularly at higher cycles.

Problems with failures in the tab area were common with unidirectional specimens, and clear tab failures were deleted from the plotted data. Edge splitting was also a common problem, as misaligned fibers were cut along the specimen edges, particularly notable with Material L but also a problem with A and B [9]. Splits often occurred early in the lifetime, so that most of the lifetime was consumed with a reduced cross-sectional area and other complications such as nonsymmetry. The tabs often showed some delamination as well, particularly where the splits reached the tab area. The unidirectional materials showed some matrix cracking normal to the stress direction, particularly along the stitch lines; this was also observed in the run-out specimens.

As noted earlier, Eq. (1) has an empirical basis in a broad range of materials with well aligned fibers, where b=0.1 for E-glass strands and composites. Eq.(2) is generally applicable where the lifetime is associated with growing cracks, as in delamination studies [8], where Eq. (3) describes the crack growth behavior. Delamination tests on Materials H and J [9]0 produce a power law behavior following Eq. (3), with the same exponent, m=13.5, which fits the unidirectional S-N data well. This observation implies that the lifetime of the unidirectional materials is dominated by the matrix crack growth, edge splitting process. However, the data in Fig. 1 are also not far from the expected trend of Eq. (1) with b=0.1, and more high-cycle data will be required to adequately test either prediction.

Extrapolation to 10^9 cycles of the trend lines given in Figs. 1 & 2 for Eqs. (1) vs. (2) shows a great deal of sensitivity to the assumed model. The expected stress or strain level to produce 10^9 cycle failures is only half as great if Eq. (1) is assumed, as compared with Eq. (2). Again, more high-cycle data are required before a 10^9 cycle stress or strain level can be projected with any confidence.

Triaxial Reinforcement

Materials F/G, H/J, M and N contain 0/$\pm$45 layers of reinforcement with differing stacking sequence, relative amounts of 0 and $\pm$ 45 material, and strand sizes. These materials showed consistently poorer fatigue resistance than did the unidirectional materials. Figure 3 compares S-N data for all of the triax materials on a normalized stress plot. Despite the differences in matrix, manufacturing, and percent 0^0 material, all of the data sets overlap, and all show a clear flattening trend at high cycles. The F/G and H/J data shown are for specimens without ply terminations (joints or tapers) in the gage section, or for specimens which fail away from the ply terminations.

The triax materials showed distinctly different failure patterns from the unidirectional materials. Figure 4 shows failed triax specimens. Generally, the $\pm$ 45^0 layers failed separately, and may delaminate from the 0^0 material [9]. No significant tab problems were observed with most of these materials, and failures were usually in the gage section. The

failure sequence usually showed cracking in the $\pm 45^0$ layers, often associated with matrix cracks normal to the load in matrix rich areas around the 0^0 material. Prior to total failure, local damage zones were observed to nucleate and grow. For F/G materials these appear as in Fig 4a, while more distinct failures along with stitch lines were seen in Materials M and N. These zones often, but not always, initiated at the edges. The failure zones in Materials M and N included cracks along the $\pm 45^0$ strands and broken 0^0 strands right at the fabric stitch lines (Fig. 4(b))[9].

Strain Data

Figure 5 compares higher cycle strain data for the unidirectional and triax mate-rials. The initial strains for the unidirectional materials were in the range of 0.8% to produce failure at 10^7 cycles, while for the triax materials the strain was in the range of 0.3 to 0.4%. The latter range is already well below the extrapolated unidirectional strains at 10^8 to 10^9 cycles. The triax results are very disappointing in terms of allowable strain levels. Also notable on Figure 5 are data for the N triax tested in the transverse direction, (90/$\pm$ 45). These failure strains are in the same range as for the 0^0 direction. It is apparent that all of the triax materials fail soon after the $\pm 45^0$ layers crack, and are not dominated by the 0^0 layer strain capability.

An approximate prediction of what should happen when the $\pm 45^0$ layers fail can be obtained from classical laminate theory [9]. If the $\pm 45^0$ ply stiffness is then assumed to be zero, in Materials M and N, for example, the overall modulus should decrease by about 25%, raising the strain on the 0^0 material by a factor 1.25. From Figure 5, even the extreme assumption of zero stiffness in the cracked plies, $\pm 45^0$ ply failure should not lead to the observed failure of the 0^0 layers at the lower strain levels. As noted in ref. 8, carbon fiber composites fabricated from prepreg tend to follow to 0^0 ply fatigue trends under these conditions. Thus, the triax performance in tension is much poorer than expected either from experience with other composites or from simple calculations. Current modelling of this problem suggests that matrix and off-axis cracks generate much higher stress concentrations in the 0^0 E-glass materials than for carbon/epoxy. This is particularly significant when the off-axis material is bound very tightly to the off-axis plies.

Complex Laminate Structures

Material P is a more complex laminate constructed of layers of triax, mat, and unidirectional material (about 50% unidirectional). Figure 6 compares the fatigue trend for material P with that of the pure triax materials. The failure mode for this laminate showed initial fracture zones in the triax like Fig. 4(b), followed by delamination from the undirectional layers. While this appears to be the desired failure sequence to protect the more structural and fatigue resistant unidirec-tional layers, the normalized lifetime trend and failure strains were similar to those of the other triax materials [9]. This disappointing result again indicates the need for improved modelling and more fatigue resistant triax rein-forcement.

Specimen Edge Effects

Figures 7 and 8 give S-N data for materials T and V and U and W, respectively. These are comparisons of standard coupons of two different triax materials with special coupons fabricated without cut edges (all specimens were 2-inches wide). The latter specimens were molded with the triax wrapped at the edges to prevent cut edge effects. No significant difference was observed in either the lifetime data or the failure modes when the wrapped edges were used. Similar test comparisons are being carried out with unidirectional materials. The results given here suggest that conventional material coupons may give results which are not significantly affected by the presence of free (cut) edges, for triax reinforcement.

Compression and Reversed Loading

Compression and reversed loading fatigue tests have been carried out on materials N and P, containing triax and triax/mat/unidirectional rein-forcement. These tests were exploratory in nature, but provide meaningful trends for the geometries and constraint conditions used. Compression tests are recognized [2] as producing results which depend on the test conditions, such as buckling restraints, load introduction details, and thickness. The tests represented here, used tabbed coupons clamped in hydraulic grips with no lateral gage section restraints. Gage lengths of 1/4 to 1.0 inches prevented elastic buckling at the maximum compressive load, but out-of-plane deflections were commonly observed after damage was well developed (close to the failure condition). Static data showed that the static strength in compression was significantly (up to 50%) higher if the thickness was doubled. Thus, caution must be used in interpretation these results.

Figures 9 and 10 show the S-N data for materials N and P at R values of 0.1 (tension-tension), -1.0 (reversed), and 10 (compression-compression). The static compression strengths are lower than for tension, but the compression fatigue trends are less steep than for tension (b is higher in Eq. (1)). The values of b observed in compression are similar to literature data for other glass and carbon fiber composites [8]. Reversed loading results generally follow the lower of the tension or compression trends for the cycle range in question, with a slightly reduced lifetime as compared to the pure tension or compression curve. The data in Figs. 9 and 10 suggest a transition from compression to tension dominated failures as the cycles-to-failure increase and the stress level decreases. This observation is particularily relevant to bending conditions in blade tests or service loading.

Comparison With Other Studies

Several wind energy related programs in Europe have reported significant fatigue data for materials of the general type studied here [10-14]. Data for unidirectional fiberglass composites in tensile fatigue (R=0.1) show failure strains in the 10^6 to 10^8 cycle range which are very similar to those in this study, around 0.8% at 10^7 cycles [10,11]. The S-N data

for predominantly unidirectional material at R = 0.1 in Ref.11 approximately follow Eq. (1) with b# 0.1, with the data falling slightly above the predicted lifetimes (with some uncertainty about the static test load rate effects). No fatigue limit is found out to 10^8 cycles. Data for spectrum loading (WHISPER spectrum) are reasonably predicted by a linear damage law combined with the constant amplitude results. However, testing at two stress levels tended to extend the life at the second (lower) level, contrary to linear damage expectations. Reversed loading (R= -1) produces lower failure stress levels, but is presumably related to the nature of any bucking constraints in compression.

Results in Ref. 12 were generally similar to those found here in trend and strain levels for unidirectional material at R= 0.1. Compression data and R= -1.0 data are generally at similar strains to those in Ref. 10, despite the use of an antibuckling device which appeared to raise the static compressive values. Spectrum fatigue results (WHISPX) showed approximate agreement with linear damage law predictions in tensile dominated fatigue, but less agreement in compression [13].

With regard to the effects of vinylester vs. polyester matrix materials, data in Ref. 14 support the findings in the present study. Materials with woven roving and mat reinforce-ment showed some advantage for vinylesters over orthopthalic polyesters at high stresses (above where matrix cracking occurs on the first cycle), but S-N data (R= -1.0) for all matrix systems converged at lower stresses/longer life-times. This has also been observed in automotive SMC composites with various matrix modifications [8]. Data reported in Ref. 15 for flexural fatigue appear to show similar convergence at high cycles for vinlyester and polyester matrices, but the vinylester showed a greater advantage at lower cycles than found in other data sets.

CONCLUSIONS

The unidirectional materials performed close to expected trends despite significant fiber misalignment; a power law trend appears to provide the best fit to most of the data. This fit may imply that the lifetime is dominated by matrix cracking along mis- oriented fibers, as the power law exponent correlates with the exponent obtained in ply delamination tests. Triaxial materials showed a steep S-N data trend at higher stresses, which tended to flatten at lower stress. Data from several material types with differing matrix (vinylester and polyester), percent of 0^0 fibers, and manufacturing method could be normalized to a single S-N curve. Failure of the triaxial material appears to be dominated by cracking in the $\pm 45^0$ plies, which was not anticipated. Data are also given in Ref. 9 for changes in laminate stiffness and temperature during cycling.

Results for more complex laminates containing uniaxial as well as triaxial plies showed a triax-dominated be-havior in tension. Compression fatigue produced a lower static strength, but also less fatigue sensitivity, than for tension. Reversed loads followed the lower of the tension or compression trend lines. Special triax coupons with wrapped edges showed similar results to coupons with machined edges.

References

1. "Assessment of Research Needs for Wind Turbine Rotor Technology", Report of the Committee on Assessment of Research needs for Wind Turbine Rotor Materials Technology, National Research Council, National Academy Press, Washington D.C. (1991).

2. "Life Prediction Methodologies for Composite Materials", Report of the Committee on Life Prediction Methodologies for Composite Materials Advisory Board, NRC, National Academy Press, Washington D.C. (1991).

3. K.L. Reifsnider, Ed., Fatigue of Composite Materials, Vol. 4 Composite Materials Series, Ed. R. B. Pipes, Elsevier Publishing Co., London (1991).

4. A.H. Chardon and G. Verchery, Eds., Durability of Polymer Based Composite Systems for Structural Applications, Elsevier Applied Science, London (1991).

5. J.F. Mandell, "Fatigue Behavior of Fiber-Resin Composites", Developments in Reinforced Plastics-2, G. Pritchard, Ed., Applied Science Publishers, London, p. 67 (1982).

6. R. Talreja, "Fatigue of Composite Materials", Technomic, Lancaster, PA (1987).

7. M.J. Owen, In Short Fiber Reinforced Composite Materials, ASTM STP 772 B. A. Sanders, Ed., ASTM, Phil. p. 64 (1982).

8. J.F. Mandell, "Fatigue Behavior of Short Fiber Composite Materials", The Fatigue Behavior of Composite Materials, K.L. Reifsnider, Ed., Ch. 7, Elsevier Science Publishing, London (1991).

9. J.F. Mandell, R.M. Reed, and D.D. Samborsky, "Fatigue of Fiberglass Wind Turbine Blade Materials," Contractor Report SAND92-7005, Sandia National Laboratories, Albuquerque, N.M.

10. P.W. Bach, "High Cycle Fatigue Testing of Glass Fiber Reinforced Polyester and Welded Structural Details" , ECN Report C-91-010, ECN, Petten, The Netherlands (1991).

11. R.H.F. Tikkemeijer and P.A. Joosse, "Fatigue of Wind Turbine Materials", NOVEM Contract 24.300/0550, NOVEM Utrecht, 3503 R.E. Utrecht, The Netherlands (1991).

12. Ch. W. Kensche and T. Kalkuhl, "Fatigue Testing of GL-EP in Wind Turbine Rotor Blades", Proc. European Community Wind Energy Conf., Madrid (1990).

13. Ch. W. Kensche, Institute for structure and Design, DLR Stuttgart, Germany, Personal Communication (1991).

14. A.T. Echtermeyer, L. Buene, B. Engh, and O.E. Sund, "Significance to Damage Caused by Fatigue on Mechanical Properties of Composite Laminates", Proc. ICCM 8, Honolulu (1991).

15. P. Burrell, T. McCabe, and R. de la Rosa, "Cycle Test Evaluation of Various Polyester Types and a Mathematical Model for Projecting Flexural Fatigue Endurance," Proc. 41st Ann. Tech. Conf. Reinforced Plastic/Composite Inst., Society of the Plastics Industry, Paper 7-D (1986).

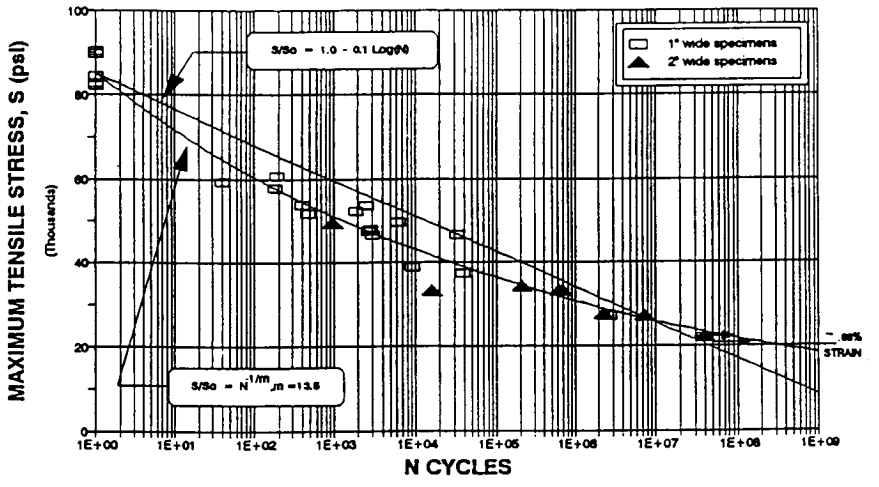

FIGURE 1 S-N Data For Material B (Unidirectional)

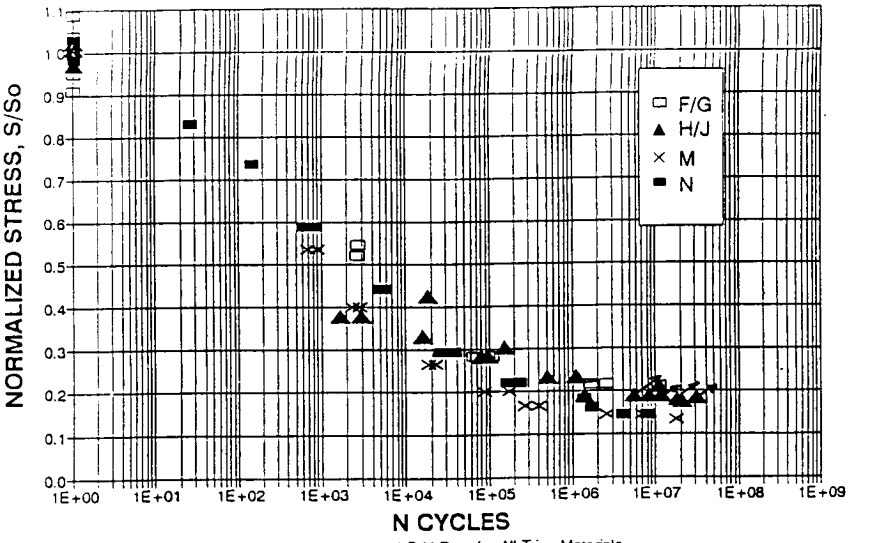

FIGURE 3 Normalized S-N Data for All Triax Materials

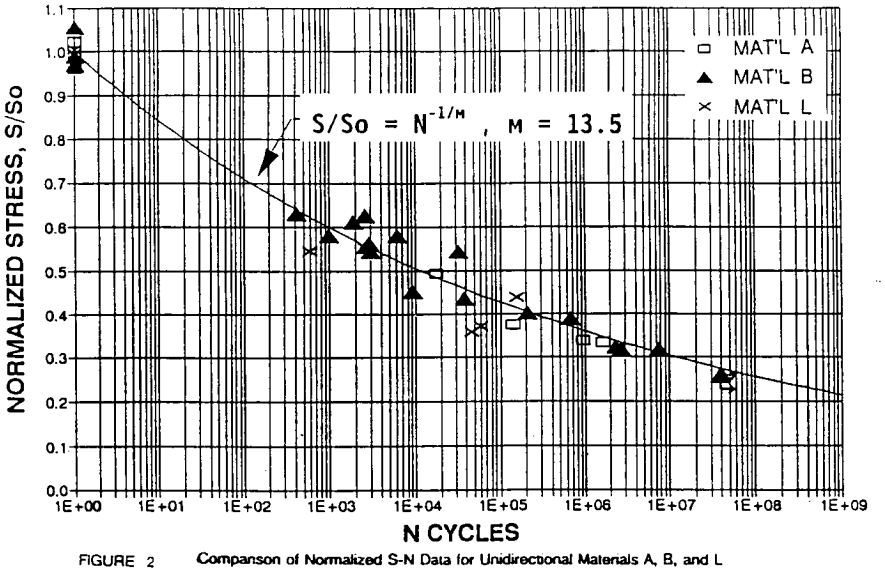

FIGURE 2 Comparison of Normalized S-N Data for Unidirectional Materials A, B, and L

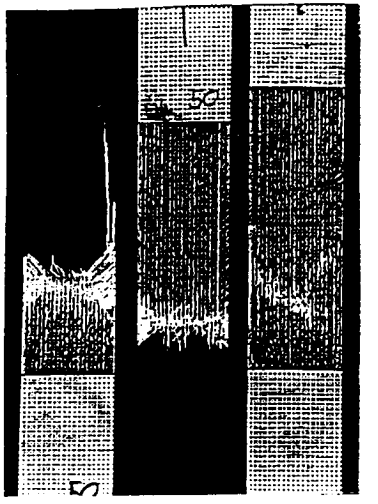

FIGURE 4a Damage Growth and Failure, Materials F/G

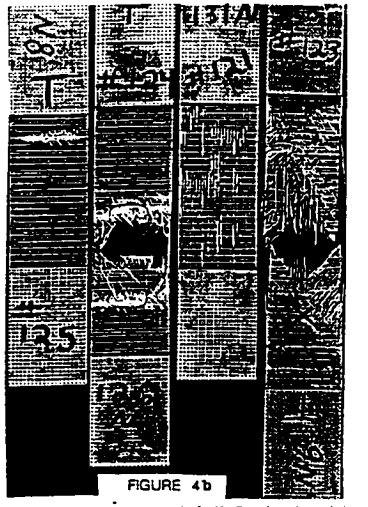

FIGURE 4b

Typical [0/±45] Material N Scrim Cracking, and ±45 Damage Region Failure Modes.

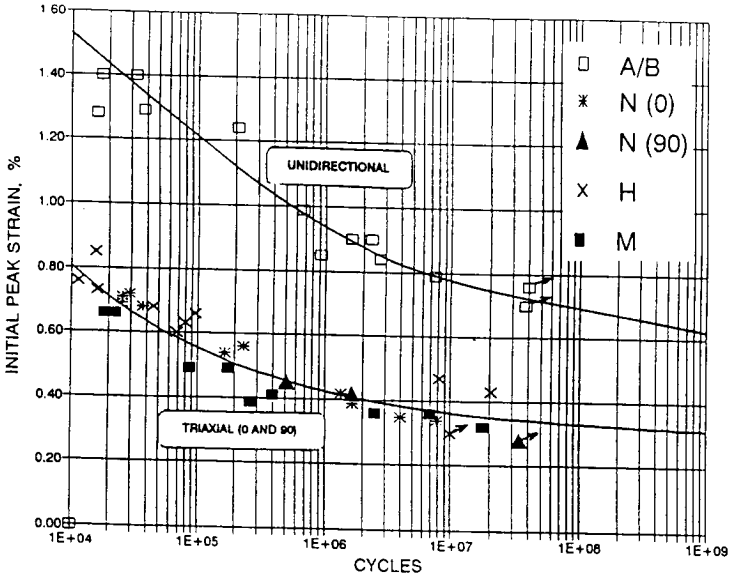

FIGURE 5 Initial Strain vs. Cycles to Failure, Unidirectional and Triaxial Materials

FIGURE 7 TRIAX NORMALIZED DATA FOR MATERIALS U AND V AT R = 0.1

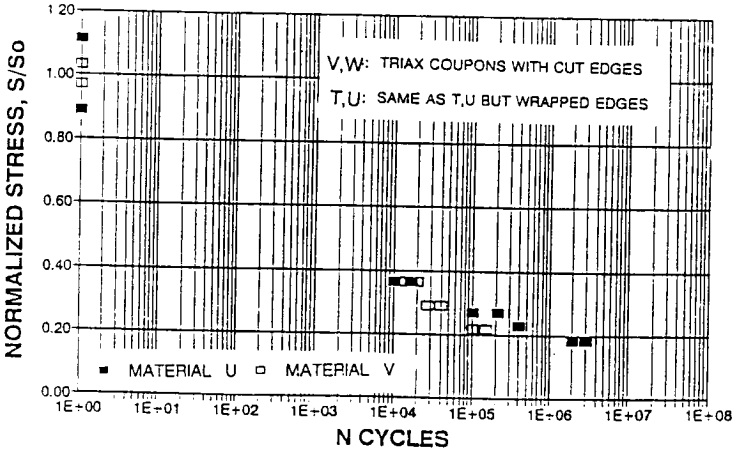

FIGURE 6 TRIAX DATA FOR MATERIALS M, N AND P AT R = 0.1

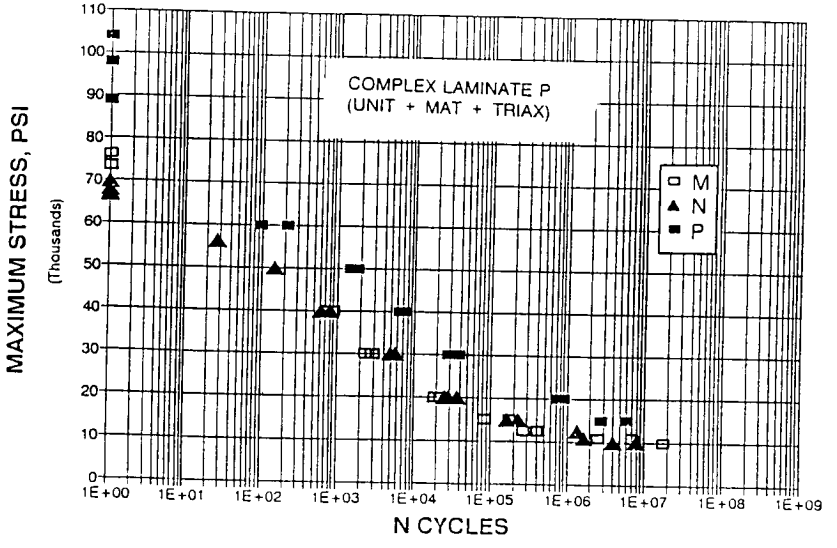

FIGURE 8 TRIAX NORMALIZED DATA FOR MATERIALS T AND W AT R = 0.1

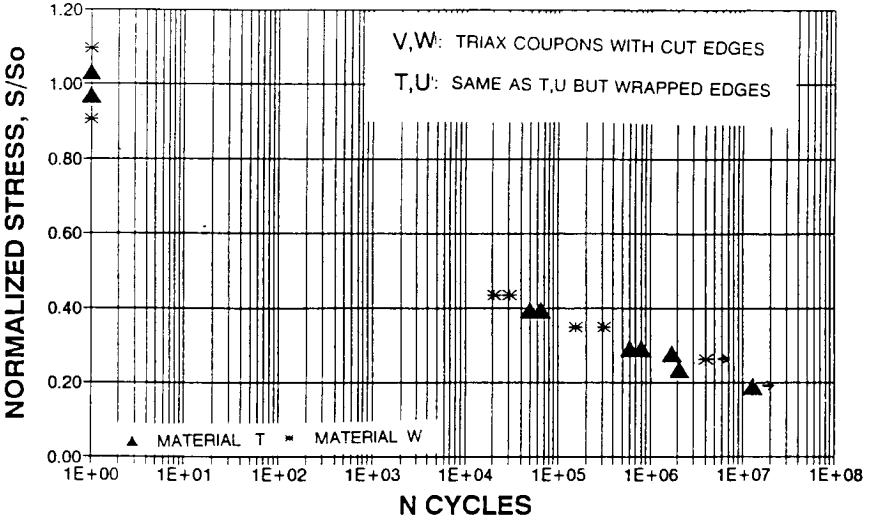

TABLE 1

FIBERGLASS MATERIALS TESTED

MATERIAL	V_f	PLY GEOMETRY	MATRIX	THICKNESS (INCHES)	LOAD DIRECTION	DESCRIPTION
A	0.30	$[0]_5$	polyester	0.16	0°	12 oz unidirectional fabric
B	0.30	$[0]_5$	vinylester	0.16	0°	12 oz unidirectional fabric
F	0.36	$[(\pm45/0)_n]_s$	polyester	0.19/0.28	0°	33 oz Triax (48% 0's,26% +45's, 26% -45's) 6 plies reduced to four at central ply termination
G	0.36	$[(0/\pm45)_n]_s$	polyester	0.19/0.28	0°	Same as material F
H	0.37	$[(\pm45/0)_3]_s$	polyester	0.25	0°	32 oz Triax (70% 0's, 15% +45's, 15% -45's) 6 plys with ply joint in central 2 plys
J	0.37	$[(0/\pm45)_3]_s$	polyester	0.25	0°	Same as material H
L	0.50	$[0]_n$	polyester	0.13	0°	Non-woven uniaxial fibers
M	0.38	$[0/\pm45]_n$	vinylester	0.15	0°	Triaxial reinforcement (Same percentages as F)
N	0.38	$[0/\pm45]_n$	polyester	0.15	0°, 90°	Same as material M
P	0.40	[T/M/U/M/T]	vinylester	0.15	0	Combined (0/+-45) Triax(T), chopped strand mat(M) and unidirectional(U) plies.
R	0.39	$[0/\pm45]_n$	polyester	0.14	0	Separate 0° and ±45° plies. 50 % 0, 50 % ±45

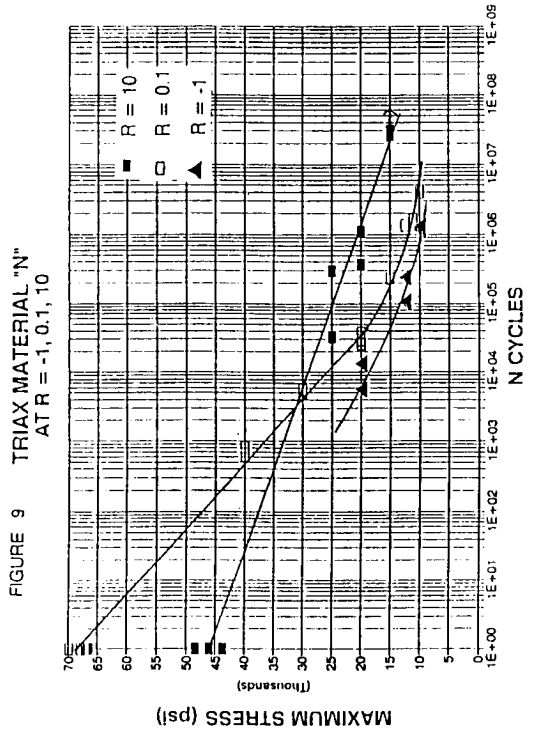

FIGURE 9

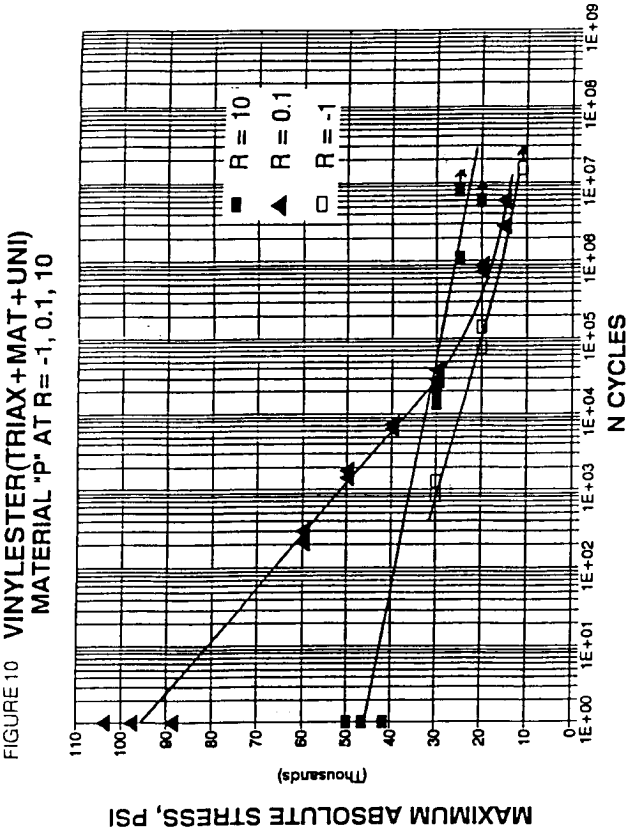

FIGURE 10